Published in final edited form as:
Brain Res. 2009 January 9; 1247: 100–113. doi:10.1016/j.brainres.2008.09.084.

Corticolimbic Mechanisms in the Control of Trial and Error Learning

Phan Luu[1,2], **Matthew Shane**[3], **Nikki Pratt**[4], and **Don M. Tucker**[1,2]

1 *Electrical Geodesics, Inc., 1600 Millrace Dr. Suite 307, Eugene, OR 97403*

2 *Department of Psychology, University of Oregon, Eugene, OR 97403*

3 *The MIND Institute, 1101 Yale Blvd NE, Albuquerque, NM 87131*

4 *University of Louisville, Psychological & Brain Sciences, Louisville, KY 40292*

Abstract

As learning progresses, human and animal studies suggest that a frontal executive system is strongly involved early in learning, whereas a posterior monitoring and control system comes online as learning progress. In a previous study, we employed dense array EEG methodology to delineate the involvement of these two systems as human participants learn, through trial and error, to associate manual responses with arbitrary digit codes. The results were generally consistent with the dual-system learning model, pointing to the importance of both systems as learning progressed. In the present study, we replicate and extend the previous findings by examining the brain responses to error trials as well as examine the activity of these two systems' response to feedback processing. The results confirmed the role of these two systems in learning but they also provide a more complex view of their makeup and function. The frontal system includes ventral (inferior frontal gyrus, ventral anterior cingulate cortex, anterior temporal lobe) corticolimbic structures that are involved early in learning whereas the posterior system includes dorsal (anterior and posterior cingulate and medial temporal lobe) corticolimbic circuits that are engaged later in learning. Importantly, the engagement of each system during the course of learning is dependent on the nature of the events within the learning task.

Keywords

Event-related potential; ERP; Learning; Medial Frontal Negativity; Feedback-Related Negativity; MFN; P300; Expertise; Action

1. INTRODUCTION

Regulating behavior requires learning appropriate actions in the context of environmental events. The outcome of successful learning reflects the integrated function of self-regulatory processes (such as regulation of motives, action monitoring, memory encoding and retrieval etc.) that are controlled by specific corticolimbic networks. Electrophysiological and imaging

Corresponding Author: Phan Luu, Electrical Geodesics, Inc., 1600 Millrace Dr. Suite 307, Eugene, OR 97403, (541) 687-7962, Fax: (541) 687-7963, email: pluu@egi.com.

studies have converged to identify diffferential engagement of these networks during different stages of learning. For example, the prefrontal lobes (including the inferior frontal gyrus, dorsolateral prefrontal cortex, and medial prefrontal cortex), and anterior cingulate cortex (ACC) have been observed to be strongly engaged early in the learning cycle when stimulus-response mappings are actively being established (Chein & Schneider, 2005; Luu, Tucker, Stripling, 2007; Toni et al., 1998). In later stages of learning, however, once contingency mappings have become consolidated, these frontal structures exhibit a reduction in activity. In contrast, posterior regions, including the posterior cingulate cortex (PCC), precuneus, cuneus, superior parietal lobule, and intraparietal sulcus demonstrate increased activity during these later stages (Chein & Schneider, 2005; Luu et al., 2007; Toni & Passingham, 1999). The reduction of activity observed in frontal structures in later stages of learning appear to represent reduced reliance on top-down control systems once learning has been established, while the increased activity observed in posterior structures may represent the establishment and automatization of the learned action patterns as well as continued monitoring of performance (Chein & Schneider, 2005; Toni & Passingham, 1999).

These findings, based on human studies, are consistent with animal research identifying two separable circuits underlying discriminative learning: one that supports the rapid acquisition of new skills through regulation of ‘executive’ control systems, and a second system that supports the habitual automatization of learned behavior (Gabriel et al., 2002). These two systems allow learning to be graded: moving from intensive monitoring and control early in the learning cycle, when stimulus-response contingencies remain undeveloped, to reduced reliance on these resource-demanding processes and automated performance once these contingencies have been sufficiently mapped (see Gabriel et al., 2002 for additional discussion). Bringing the animal learning model to human learning studies, we hypothesized that initial learning requires greater executive control from frontolimbic networks, whereas in later stages of learning, when performance becomes more automated, processing in posterior corticolimbic networks dominates both performance and the continued adjustments of learning (Luu et al., 2007).

In that research, we examined the activity of cortical and limbic systems during visuomotor learning in humans using dense-array EEG methodology. The task employed is amenable to automated performance once learning has been achieved because the stimulus-response mappings are constant (see Chein & Schneider, 2005). We found that posterior cortical regions (including parietal, PCC, and parahippocampal cortices, as indexed by the P3) became progressively engaged as participants discovered and learned stimulus-response mappings (Luu et al., 2007). However, the pattern of neural activity in learning was more complex for frontal components. We identified a frontal component of the averaged event-related potential (ERP) that was localized to ventral corticolimbic networks (anterior temporal pole and inferior frontal cortex). Furthermore, this component was lateralized according to the stimulus (to the left frontal lobe for digit codes and to the right frontal lobe for spatial locations). The analysis showed that, although it could be confused with the inferior dipole inversion of the P3 or “Late Positive Complex”, this component showed not only a unique source but a unique time course as well.

We described this component as the Lateralized Inferior Anterior Negativity (LIAN). Although the LIAN was differentially lateralized for verbal and spatial stimuli, it showed a gradual deactivation during learning only for spatial location-response mappings. Under the hypothesis that early control of learning engages greater control from frontal executive networks, we would predict that the decrease in the LIAN after learning would be observed for both the digit code and spatial pattern learning conditions. On the other hand, a right-lateralized frontal decrease with learning is consistent with a meta-analytic study, based on fMRI findings that

revealed right-lateralized biases for learning-related deactivations of the lateral ventral prefrontal cortex (Chein & Schneider, 2005).

In contrast, the LIAN for digit-response mappings showed a slight, although not significant, increase as learning progressed. A possible explanation for the sustained LIAN after learning is that participants may not have achieved automated levels of performance. A second explanation, though not exclusive of the first, involves the observation by Chein and Schneider (2005) that the left ventral prefrontal cortex remains strongly engaged during practice performance of word pair association tasks, which suggested to them that this region may be involved in representational functions that are not immediately associated with cognitive control.

In the Luu et al. (2007) study, we also examined a component reflecting activity in dorsal frontolimbic networks, described as the medial frontal negativity (MFN), localized to the medial prefrontal cortex, including the ACC. The MFN has been shown to be important to aspects of the executive monitoring of the learning process (Gehring & Willoughby, 2002). The hypothesis that frontal control decreases as learning progressed was not supported by the measures of the MFN in the Luu et al. study; the MFN actually increased as subjects gained knowledge of the correct stimulus-response mapping, and as they demonstrated consistent performance guided by this knowledge.

In the present study, we replicated and extended the findings by Luu et al. (2007) in a separate sample of subjects. The replication involves analysis of target-locked brain responses on correct trials. The extension involves analysis of target-locked brain responses to error trials and feedback-locked brain responses. The analysis of target-locked brain responses on error trials permits further examination of the nature of the MFN increase we previously observed. The analysis of feedback-locked responses will permit determination of how corticolimbic structures involved in learning are affected by informational content, providing us with a more complete picture of how their activity is moderated during different learning stages.

Based on our previous explanation that the MFN increase may reflect development of action context representations (thus leading to opportunities for response conflicts), we predict that target-locked MFN amplitudes would be particularly large for error trials that occur after learning. We hypothesize that activity of the frontal circuit (i.e., fast learning system) would be reduced in response to feedback as learning progressed because the accuracy of actions are internally represented once learning is established (see Holroyd & Coles, 2002). Specifically, we predict the feedback-related negativity (FRN; Luu, et al., 2003), which indexes frontolimbic evaluative mechanisms, would decrease in amplitude with learning. Similarly, we predict that the LIAN would appear in evaluation of the feedback to integrate the response outcome during the learning process (see Passingham, Toni, & Rushworth, 2000) and would decrease with learning. In contrast, we hypothesized that activity of the slow learning system in the posterior brain (as indexed classically by the P3 response) would show a decreased response to correct feedback as learning progresses (reflecting less context-updating) but not a decreased response to error feedback. The logic is that context updating processes (Donchin & Coles, 1988) remain sensitive to context violations such as errors[1].

[1]In this paradigm, the feedback was given immediately after the response. Therefore, the error-related negativity (ERN) precedes all of the feedback-locked ERP components that were analyzed in this study. However, it is noted that the ERN does not temporally overlap with any of the feedback-locked ERP components that were analyzed. The aims of the research reported in this manuscript are to examine learning-related changes associated with processing of target and feedback stimuli as predicted by the dual-system learning model rather than error monitoring per se. Therefore, analyses were not performed on the ERN.

2. RESULTS

Behavioral Findings

Mean number of trials required for participants to learn was 13 (SD = 6). The median reaction times for Go trials were cast into a 2 (Accuracy: Error, Correct) × 2 (Learning: Pre-Learn, Post-Learn) within-subject ANOVA, which revealed Accuracy ($F(1,10) = 21.887$, $p=0.001$) and Learning ($F(1,10) = 6.522$, $p=0.029$) main effects, indicating that reaction times were longer on error trials (mean = 1065 ms, SD = 130 ms) compared to correct trials (mean = 922 ms, SD = 111 ms), and on Pre-Learned trials (mean = 1029 ms, SD = 128 ms) compared to Post-Learned trials (mean = 959 ms, SD = 144 ms). An Accuracy by Learning interaction ($F(1,10) = 7.382$, $p=0.022$) revealed that reaction times decreased for correct responses after learning but not for error responses (Figure 1). That is, error responses had about the same reaction time before and after learning. These results are consistent with our previous findings (Luu et al., 2007).

Because participants determined how long they examined the feedback stimulus before they performed the next trial, the duration that they attended to each of the positive and negative feedback signals could be assessed. Feedback duration was submitted to a 2 (Accuracy: Error, Correct) × 2 (Learning: Pre-Learn, Post-Learn) within-subject ANOVA. One participant never responded to remove the feedback screen and the feedback remained for the full ten seconds. The analysis (n=10) revealed that participants spent a longer time viewing the feedback before they learned, compared to after they learned the task, $F(1,9) = 7.884$, $p=0.03$, consistent with reduced need for the feedback once contingencies were learned. No other main effects or interactions reached significance. Again, these results are consistent with those reported previously (Luu et al., 2007).

To define skilled performance on the task after learning the stimulus-response mappings, we computed the coefficient of variation (CV, Segalowitz & Segalowitz, 1993), which is the ratio of the standard deviation (SD) to the median reaction time (RT, CV = SD/RT). The logic is that controlled processes, such as those required early in learning, are inherently more variable than those processes responsible for automatic performance. Therefore a reduction in controlled processes should result in a reduction in the CV. For this analysis, CV values were only obtained for correct responses. Post-Learn trials were grouped into four equal bins to provide multiple measures of the post-learning performance. Within each bin, the RTs were sorted and the values for those RTs in the top and bottom 10% of the RT distribution (i.e., the tails) were set to the 10th percentile. This procedure removes extreme values at both ends of the RT distribution to provide a more stable SD measure (Wilcox, 1997). The data were submitted to a trend analysis with Learning (post1, post2, post3, post4) as a factor. The analysis revealed a significant linear trend, $F(1,10) = 18.1$, $p < .01$ (Figure 1).

Target-Locked ERP Findings

For the scalp potential ERP analyses, the channel groups used to characterize each of the major components (for target-locked and feedback-locked averages) are identified in Figure 2. The statistical analyses were performed on the scalp data with these channel groups. Source localization (using all 128 channels) for each component is provided in each figure.

MFN—Figure 3 shows the waveform for target- locked data at FCz. As can be seen, there is a clear negative deflection that peaks approximately 320 ms after target onset, closely resembling the latency and topography of MFNs identified in other studies (e.g., Gehring & Willoughby, 2002). We quantified the MFN at four channels, including FCz (see Figure 2). The MFN was defined as the difference between the most negative peak between 230–370 ms after target onset (Gehring & Willoughby, 2002;Luu et al., 2003) and the most positive preceding peak (P2, 140–280 ms after target onset). Both peaks were averaged over a 44 ms

interval centered around that peak (inclusive). The MFN measure was averaged across all four channels. Source localization (from all 128 channels) examined the major contrast between pre-learn error and post-learn error conditions. This difference provided maximal contrast with regards to peak amplitude as well as functional contrast (development of action context and response conflict, see Discussion). The results showed frontal midline sources for the MFN, including dorsal ACC and medial frontal gyrus, as well as secondary sources in the mid-cingulate and precuneus. The source orientation vectors (dark lines for each voxel) show the net dipole moment (positive direction) for each voxel, and allow the source results to be related to the potential fields in the scalp maps (e.g., the positive-down direction of the source orientation vectors for the medial frontal sources in Figure 3C are consistent with the surface-negative midline scalp potential pattern in Figure 3B).

For the MFN, a 2 (Accuracy: Correct, Error) × 2 (Learning: Pre, Post) within-subjects ANOVA revealed a main effect of Learning, $F(1,10) = 8.8$, $p < .02$, indicating that MFN amplitude is larger for Post-Learn trials. A significant interaction between Accuracy and Learning showed that the MFN differed the most between Pre- and Post-Learn error trials, $F(1,10) = 5.0$, $p < .05$ (see Figure 2).

LIAN—Figure 4A shows the LIAN at FT9 (channel 38) and FT10 (channel 121, see Figure 2). The LIAN to targets was defined as the average amplitude between 250–700 ms post-target at inferior fronto-temporal sites (refer to Figure 2 for channel cluster), referenced to a 400 ms average of the baseline period. A 2 (Accuracy: correct, error) × 2 (Learning: Pre-Learn, Post-Learn) × 2 (Laterality: left, right) within-subjects ANOVA revealed a trend for a Laterality main effect, $F(1,10) = 4.29$, $p = .07$, showing that the LIAN was of greater amplitude over the left-hemisphere. No other main effects or interactions reached significance. Figure 4B shows primary sources for the LIAN in the left inferior frontal gyrus and left temporal pole.

P3—The P3 or Late Positive Complex (LPC) to target stimuli was quantified as the average amplitude between 300 and 700 ms after target onset, referenced to the average of the 400 ms baseline (see Figure 5A). This was accomplished for left, midline, and right recording sites (see Figure 2). The data were analyzed with a 2 (Accuracy: Error, Correct) × 2 (Pre-Learn, Post-Learn) × 3 (Location: Left, Right, Midline) within-subjects ANOVA model. The results revealed a significant main effect for Location, $F(1,10) = 6.8$, $p < .03$, indicating that P3 amplitude was largest at midline recording sites. Although Figure 5 shows that the error trials are associated with the largest P300 amplitude and that correct trials after learning have larger amplitudes than correct trials prior to learning, none of these differences reached statistical significance.

Sources for the target-locked P3 were identified in the caudal aspects of the medial wall of the hemispheres (including the PCC, precuneus, and cuneus), bilateral medial temporal lobes (including the parahippocampal gyrus, see Figure 5B), and left temporal gyrus. These source results are similar to those we obtained for target-locked P3 in previous research with this paradigm (Luu et al., 2007).

Feedback-Locked ERP Findings

Feedback-Related Negativity—Except for the correct-post-learning condition, the feedback-locked waveforms do not show a clear negative peak at FCz during the 270–350 ms post stimulus interval (see Figure 6). This is unlike the target-locked data, which shows a clear MFN at this time for all conditions. Rather, for the feedback-locked data the P2 peak appears to be extended. However, at Fpz, a negative peak, preceded by a positive (P2) peak, can be observed. Compared to the target-locked MFN, the latency of this negativity is slightly delayed. We call this the Feedback-Related Negativity (FRN, Luu et al., 2003) because it behaves in a

manner consistent with previous reports (i.e., it is most negative for error feedback, particularly prior to learning, Müller, et al., 2005;Holroyd & Coles, 2002).

The FRN was defined as the difference between the most negative peak between 240–400 ms after feedback onset and the P2 (140–280 ms after feedback onset) at four frontal polar channels (see Figure 2). For each peak, data were averaged over a 44 ms interval around the peak (inclusive) prior to obtaining the difference. This difference was averaged over the four channels to provide one measure of the FRN. To explore this effect at more mediocentral sites, we applied the same criteria to sites used for quantification of the MFN. A 2 (Accuracy: Correct, Error) × 2 (Learning: Pre-Learn, Post-Learn) repeated-measures ANOVA model was used in both analyses.

Results from frontopolar sites revealed significant main effect for Accuracy, $F(1,10) = 17.4$, $p < .01$, and a trend for Learning, $F(1,10) = 3.9$, $p < .08$. The Accuracy main effect showed that error feedback was associated with the largest FRN amplitude. The Learning main effect showed that the FRN was reduced after learning. Means of the FRN for pre-learn error and post-learn error trials reveal that the FRN is more negative for error pre trials (consistent with previous findings, Müller, et al., 2005; Holroyd & Coles, 2002), although this difference was not significant. At the mediocentral sites, the FRN only exhibited a significant learning effect, $F(1,10) = 14.6$, $p < .01$, with post trials associated with a larger FRN.

Source estimate of the FRN was based on the difference between the pre-learned error and post-learned correct conditions, based on prior observations that pre-learned error feedback elicits the largest FRN amplitude and that the FRN amplitude decreases with learning (Müller, et al., 2005; Holroyd & Coles, 2002). The results revealed that the major sources for the FRN effect were surface-negative sources in the medial prefrontal cortex, including rostral and subgenual aspects of the ACC (BA 32, 25) and orbital frontal cortex.

LIAN—The LIAN to feedback stimuli was defined in a similar manner as the LIAN to target stimuli (see Figure 4B). A 2 (Feedback Type: Error, Correct) × 2 (Learning: Pre-Learn, Post-Learn) × 2 (Laterality: Left, Right) within-subject ANOVA revealed main effects of Laterality, $F(1,10) = 15.46$, $p < .01$, Feedback, $F(1,10) = 14.8$, $p < .01$, and Learning, $F(1,10) = 6.1$, $p < .04$. As expected, the LIAN is larger over the left compared to the right hemisphere. The Feedback effect showed that error feedback elicited a larger LIAN than correct feedback and the Learning effect showed that the LIAN was reduced after learning. There was a significant Accuracy × Laterality interaction, $F(1,10) = 5.0$, $p < .05$, consistent with the left-lateralization of the LIAN (Luu, et al. 2007), and with the reduction after learning attributed to its left inferior frontal sources. Source localization of the feedback LIAN was similar to that for the target, with sources in left anterior temporal and left inferior frontal regions (Figure 4C and D).

P3—The feedback-locked P3 or LPC had a more dorsal and rostral distribution than the target-locked P300 (see Figure 7B). Moreover, unlike the target-locked P3, there is a clear dip at approximately 500 ms after feedback onset (see Figure 7A and Kotchobey et al., 1997). Therefore, we defined the P3 at two time intervals: as the average amplitude between 300–500 ($P3_1$) ms and as the amplitude between 500–700 ($P3_2$) ms after feedback onset and referenced to the average of the 400 ms baseline. A 2 (Feedback Type: Error, Correct) × 2 (Learning: Pre-Learn, Post-Learn) × 4 (Location: Left, Right, Midline, Mediofrontal) within-subject ANOVA was conducted for each P3 measure. Geisser-Greenhouse corrections were applied where appropriate. The analysis revealed very similar results for both measures of the P3 (consistent with findings by Kotchobey et al., 1997). Therefore, we only report the results for the $P3_2$ measure.

Significant main effects for Location, ($F(3,30) = 4.9$, $p < .03$ (Geisser-Greenhouse epsilon = .57), and Feedback Type, $F(1,10) = 14.0$, $p < .01$, were obtained. The Location main effect showed that the P3 was largest at midline and mediofrontal sites. The Feedback Type main effect was qualified by a significant two-way interaction involving Feedback Type and Learning, $F(1,10) = 7.1$, $p < .03$. This interaction describes amplitude differences between error and correct feedback as a function of learning. The interaction revealed that correct feedback after learning elicited the smallest P3 response whereas error feedback elicited large $P3_2$ amplitudes, regardless of learning stage.

Although not significant, $F(3,30) = 3.0$, $p < .1$ (Geisser-Greenhouse epsilon = 4.0), a three-way interaction involving Feedback Type, Learning, and Location suggested that the difference between error and correct feedback after learning was largest along the midline and mediofrontal sites. Source estimates for the feedback-locked P3 were obtained at the peak of the $P3_2$ (~680 ms). Similar sources as for the target-locked P3 were identified, plus additional sources in the rostral aspects of the medial frontal lobes (including the ACC, see Figure 7C).

3. DISCUSSION

The behavioral and EEG data closely replicated our earlier findings on frontolimbic components in response to the the target stimulus (Luu, et al., 2007). Neither study showed a simple decline of frontolimbic activity as learning progressed. Activity in the left inferior frontal gyrus and left ventral temporal lobe and pole (as indexed by the LIAN) was strong in the early learning stage for both studies with the digit task. However, in neither study did this activity decline significantly over time in processing the target digits, as we had originally hypothesized (Luu, et al., 2007). In both the present and the previous study, the target-locked MFN, localized to the ACC, was found to increase as subjects learned. Similarly, the amplitude of the target-locked P3, indexing activity from the PCC, parietal lobe, and medial temporal lobes, also increased as subjects learned. Examination of the target-locked MFN response to error trials in the present study, we found that MFN was largest for error trials committed after learning.

The evidence of neurophysiological activity in feedback processing was consistent with the hypothesis that the frontolimbic responses to feedback, indexing the functions of the fast learning system, would be strongest during early learning and would decline as subjects consolidated the stimulus-response mappings during learning. Similarly, the index of activity in the slow learning system (P3) supported the hypothesis that the slow learning system would decrease its activity in response to correct feedback as learning progress, but would re-engage in response to error feedback. In the following sections we discuss the potential functional significance of each ERP component as it relates to the experimental conditions and the estimated underlying neural sources.

The Medial Frontal Negativity and the Feedback-Related Negativity

In addition to replicating the target-locked MFN for correct trials, wherein the amplitude of the MFN associated with correct responses becomes larger after learning, we were able to examine the target-locked MFN to error trials in the present study. These data revealed that errors after learning are associated with the largest MFN amplitudes, when monitoring requirements are expected to be strongest. The cortical source of the MFN was estimated to be in the medial prefrontal cortex (including dorsal ACC) and mid-cingulate cortex (see Figure 3). Previously, we proposed that the dorsal aspect of the ACC can be understood as tracking task relevant parameters (including valence of feedback, conflicting task demands etc., Luu et al., 2003). The present findings, as well as recent fMRI results, are consistent with this proposal.

Elliot and Dolan (1998) found that generating hypotheses to guide response selection activated the dorsal ACC. Similarly, Behrens et al., (2007) found dorsal ACC activation to be associated with making a choice (as opposed to monitoring outcomes). Using an arbitrary visuomotor association task, Eliassen et al. (2003) found that activity localized to the mid-cingulate cortex increased with learning. These researchers proposed that this activity may reflect memory or associative processes that support performance. Taken together, these findings suggest that the dorsal ACC is involved in the early representation of action contexts. That is, as subjects learn (either to make an appropriate stimulus-response mapping or to make a particular choice for a reward), a context is formed. Increased MFN amplitudes during learning appear to reflect the development of a representation of the action context that is maintained within the limbicmotor pathway to guide the ongoing monitoring of behavior. This development of action context produces the conditions necessary for conflicting response demands (see Botvitnik et al., 2004).

As actions become more automated, contextual representation appears to transfer to posterior networks, such as the PCC (Gabriel et al., 2002). According to this reasoning, in a fully automated stage of learning and action control, we would expect activity in the dorsal ACC to decrease, unless an error is committed in which case there will be a strong ACC response. In an fMRI study Toni et al. (1998) found that learning a sequence of motor responses was associated with an initial rise in dorsal ACC activation followed by sustained activity and then an eventual decline. Our hypothesis of dorsal ACC function is compatible with Rushworth et al.'s (2004) proposal that the ACC is involved in the representation action values, with Holroyd and Coles's (2002) proposal that it acts as a motor control filter, and with the conflict monitoring theory of ACC function (Botvitnik et al., 2004). By emphasizing the ACC's role in representing the context for action, we emphasize the theoretical links to the context representation supported by other dorsal cortical networks, including the PCC and hippocampus.

In this study we identified a parallel frontal component in the feedback-locked averages, the FRN. The FRN differed substantially from the MFN in terms of functional associations as well as cortical generators. The FRN was sensitive to the nature of the feedback, being more negative to error feedback, and its cortical generator was found to be in the rostroventral (subgenual) ACC (rather than the dorsal ACC). This distinction may be important, given the ventral limbic (amygdala, anterior temporal pole, and orbital frontal cortex) input to the subgenual ACC (in contrast with the greater connectivity of the dorsal ACC with dorsolateral frontal cortex, PCC, parietal lobe, and other regions of the dorsal corticolimbic pathway). Prior studies have reported that the FRN is more negative in amplitude for error feedback (or loss, Gehring & Willoughby, 2002) and decreases with learning (Holroyd & Coles, 2002, Muller et al., 2005). We replicated those functional findings, but observed that the scalp distribution in our study of the FRN is considerably more anterior than previously reported. Holroyd and Coles reported the effect to be at approximately FCz whereas Muller et al. showed that it extended to more posterior recording sites.

Our task is a straightforward learning task, in which stimulus-response mappings are constant, and all feedback stimuli are veridical. In the two previous studies mentioned, consistency of stimulus-response mappings varied and feedback could be ambiguous. These differences may explain why the FRN in the present study was localized specifically to the rostroventral ACC whereas previous research observed more dorsal and mid-cingulate activity in the FRN. In the present paradigm, because feedback provides veridical information about performance, affective responses of the ventromedial prefrontal cortex (including the rostroventral ACC) may be strongly engaged. In paradigms where stimulus-response mappings can change and/or feedback may be ambiguous, participants may dismiss the feedback as being incorrect feedback, leading to weaker affective responses to the feedback. Similarly, it is possible that in paradigms where feedback varies in a probabilistic manner, context tracking requires engagement of the dorsal ACC. This may also explain why we only find a significant learning

effect when we analyzed the FRN at more dorsal recording sites. That is, post learning trials were associated with the largest FRN because the feedback also constitutes part of the action context.

Possibly consistent with this interpretation, results from fMRI studies examining brain responses to negative feedback during probabilistic learning and estimation tasks have identified activations in the dorsal ACC (Holroyd et al. 2004, Ullsperger & von Cramon, 2003). In fMRI studies that examined brain responses to commissions of errors, both dorsal and rostroventral ACC regions were found to be active (Kiehl et al., 2000, Menon et al., 2001). Recent fRMI studies that utilized decision making (Behrens et al., 2007) and social evaluation (Somerville et al., 2006) tasks have identified rostroventral ACC activation during feedback processing. Previously, we proposed that the rostroventral aspect of the ACC is involved in the affective evaluation of action outcomes (Luu et al., 2003). The present finding with localization of the FRN is consistent with this proposal.

The Lateralized Inferior Anterior Negativity

Consistent with our previous results for digit targets (Luu et al., 2007) the LIAN in the present study was left-lateralized, and its amplitude did not differ as a function of learning. Based on the dual-learning system model (Gabriel et al., 2002) and prior research showing a shift from frontal to posterior networks with practice (Chien & Schneider, 2005), we first hypothesized that the LIAN would decrease as learning occurs. In both the previous and present studies, this was not observed as participants learned the digit-response mappings. A possible explanation for the lack of reduction in activity is that even after 800 trials, subjects have not fully mastered the task, at least to automated levels of performance. Examination of the CV data, however, revealed that subjects did demonstrate an increase in skilled performance. Therefore, the results are more consistent with Chein & Schneider's (2005) finding that the left ventral prefrontal cortex remains strongly active during practiced performance for word-pair tasks. These researchers suggested that this cortical region is involved in representational functions rather than cognitive control.

The functional significance of the LIAN in learning can be inferred from studies that have examined the role of the inferior frontal gyrus, orbitofrontal cortex, and temporal lobe in arbitrary visuomotor association learning tasks. Bussey et al. (2001, 2002) demonstrated that lesions to the ventrolateral and orbital regions of the prefrontal cortex in monkeys disrupted rapid acquisition of stimulus-response mappings; animals could still learn the task but they required many more training sessions. The authors interpreted these findings to indicate that the ventrolateral and orbitofrontal aspects of the prefrontal lobe are involved in acquiring and/or application of response strategies or response rules. An example of a response strategy or rule that can be used during visuomotor learning is lose-shift. Using this strategy, a learner would make a different choice on the next trial if the present choice results in failure.

In humans, the role of frontal and temporal regions in visuomotor learning has been attributed to memory operations, in which targets take on associative meaning (Bunge et al., 2003; Toni et al., 2001;Brovelli et al., 2007). Results from memory studies suggest that the ventrolateral prefrontal cortex is involved in memory retrieval through its interaction with temporal lobe structures, including the hippocampus (Badre et al., 2005; Simons & Spiers, 2003). Passingham et al. (2000) noted that the ventral aspects of the prefrontal lobe, including the inferior frontal gyrus, has been shown to be involved in the representation of the stimulus, the responses made to the stimulus, and the feedback (i.e., outcome) of the action. These representations are central to the learning visuomotor associations.

If the LIAN does indeed reflect integrative encoding/retrieval processes during learning rather than cognitive control, we would expect it to decrease in response to feedback presentation

after the stimulus-response mappings are learned because feedback is no longer informative. Prior to learning, feedback would be used to update and reinforce digit-response associations, but after having learned the mappings feedback is no longer required. Behaviorally, we showed that prior to learning the task, subjects viewed the feedback for an extended period of time, and after having learned the stimulus-response mappings, subjects quickly removed the feedback. In a corresponding manner, the feedback-locked LIAN declined significantly after participants learned the task.

The P3

Gonzalves et al., (1999) have proposed a template-restoration model of the for the P3, which is akin to the context-update model of Donchin and Coles (1988). In the template-restoration model a template of a stimulus (the response-mapping rules in the present study) are restored or reinforced on a trial-by-trial basis. The P3 is proposed to reflect this restoration-reinforcement process. The larger P3 amplitudes observed after learning may be explained by the findings that reductions in processing requirements are associated with enhancements of P3 amplitudes(Gonzalves & Polich, 2002). Learning results in stable representations of action context (i.e., the template). This stable representation reduces processing resource requirements (perhaps through facilitation, as shown by the decreased CV measure associated with learning), which results in larger P3 amplitudes (and enhancement of the context model) after learning. Therefore, we take the observed increases in P3 amplitude to reflect the operations of contextual maintenance processes during the later stages of learning by the posterior, slow learning system. This interpretation is slightly different than that proposed by Barceló et al. (2000) who interpreted the P3 amplitude increase with learning to reflect the acquisition of a stable representation of response-rules. An alternative explanation is that a stable representation of response-rules would decrease the latency variability of the P3 on single-trials, which would be reflected as an increase in the stimulus-locked average.

In contrast to the target-locked P3 amplitudes, analysis of the feedback-locked P3 showed that correct feedback after learning was associated with the smallest P3 amplitude, whereas error feedback elicited the largest P3 amplitude, especially after learning. Moreover, source estimation of the feedback-locked P3 revealed source generators within the medial prefrontal cortex that were not evident in the target-locked P3. Kotchobey et al. (1997) examined an informed guessing task and showed that unexpected outcomes were associated with large P3 amplitudes compared to expected outcomes (like we did, these authors found parallel results for measures of the P3 or LPC at 350 and 550 ms). They also found that subjective expectancy (i.e., participant's prediction) was not associated with amplitude differences. Therefore, they argued that processes indexed by P3 amplitude reflect rule-related expectancy violations developed from estimations of the likelihood of an event (as opposed to to subjective, predictive expectancies). This proposal is consistent with the present results. As participants learned the task, representations of the task parameters (i.e., stimulus-response mappings, feedback contingencies, etc.), which can be understood as forming rule-related expectancies, gradually develop within the slow learning system (Keng & Gabriel, 1998) and violations of the context (i.e., post learned errors) require template or contextual updating mechanisms (Donchin & Coles, 1988;Gonzalvez et al., 1999), perhaps supported by additional engagement of control processes (as reflected in the involvement of the medial prefrontal cortex).

An alternative explanation for the observed increase of the P3 amplitude for error feedback after learning is that errors are rare after learning and thus error feedback is more salient. This results in attention being allocated preferentially to error feedback, which would produce a large P3 response. The template-restoration theory of the P3 proposed by Gonzalvez et al. (1999), however, is also consistent with such an explanation. In fact, this theory has been proposed to explain the relationship between stimulus probability and variations in P3

amplitude. However, given that there was an additional medial prefrontal source associated with the feedback-locked P3, there may be additional control processes that are engaged in the update.

Limitations of the Study

We conducted this research with the first models of the HydroCel Geodesic Sensor Net design, which were 128-channel versions. Technically, source localization with 128-channel recordings is marginally accurate, compared to 256-channel recordings, even though the HydroCel 128-channel design was extended to improve the sampling of inferior (face and neck) head regions. Whereas separation of activity in frontal and posterior networks can be done with confidence with highly approximate source analysis, separating the contributions of dorsal versus ventral corticolimbic networks (Aggleton & Brown, 1999; Tucker & Luu, 2007) is theoretically critical, and for certain essential regions will require more precise source modeling. Furthermore, even though the source localizations were critical in identifying the approximate regional sources of the major components responsive to learning (FRN, LIAN, MFN, P3), the statistical analyses were conducted on the scalp reflections of these components, which are often highly superposed and thus confused. An important future methodological development will be to perform statistical analysis in source space. The present research relied exclusively on the averaged evoked (event-related) potential, when several lines of evidence suggest that important aspects of the coordination of neural networks is shown by a more dynamic analysis of the ongoing (unaveraged) EEG (Luu, Tucker, & Makeig, 2004). Also, because the EEG is generated by the cortex, which have the requisite laminar organization to generate far-field potentials, we are only able to examine cortical sources involved in learning. Yet, in many learning studies subcortical structures (such as the caudate nucleus) have been shown to be strongly engaged during learning (e.g., Grol et al., 2006, 2003; Toni & Passingham, 1999).

Perhaps most importantly, although we were able to replicate previous findings for the target-locked responses from Luu, et al. (2007), we view this line of research as still exploratory, given the limited experimental control over what monitoring or self-regulation processes are engaged at what point in the learning process. Further manipulations of motivation, learning strategy, and learning progress will be required to test the theoretical model of learning as achieved by strategic mechanisms of action regulation (Luu & Tucker, 2003).

Conclusions

The brain activity observed during the learning of a simple stimulus-response mapping involved several corticolimbic networks with differing patterns, both in processing the target stimulus that required a response and in the processing of the feedback stimulus that indicated the correctness of that response. We began with the general hypothesis of a shift in activity from frontal to posterior cortical regions as participants learned. As in our previous study, this hypothesis was inadequate in its simple form for several reasons. First, the target-locked MFN and LIAN showed increased strength as subjects gained knowledge of the task, possibly reflecting the more effective frontolimbic self-regulation that was gained in the learning process. Second, the FRN and feedback-locked LIAN did demonstrate decreases as learning progressed. Third, the feedback-locked P3, reflecting activity of posterior cortical sources, demonstrated attenuated activity in response to presentation of correct feedback and increased activity upon presentation of error feedback as learning progressed.

These electrophysiological patterns provide intriguing clues with regards to the transition from early to late learning. The results of this study emphasize that the involvement of both the early and late learning systems must be considered relative to the events within a learning trial as well as the stage of learning. For example, frontal monitoring of feedback information

decreased during the time that internal representation and monitoring processes appeared to come online. This suggests that intermediate stages of learning, as manifested by participants in this study, are characterized by intense involvement of stimulus-response mapping (LIAN), monitoring (MFN), and evaluative (FRN) functions, both as action contexts are developed (such as represented within the ACC) and as enduring representations of these contexts (P3) are formed.

EXPERIMENTAL PROCEDURES

Participants

Twenty-three undergraduates from the University of Oregon were recruited for participation. All participants had normal or corrected-to-normal vision, and reported no current drug use or medication. Only those participants who supplied at least 15 instances of each trial type (i.e., correct and error responses before and after learning occurred, see below) were included in the present analyses. Data from these eleven participants (8 male, 10 right-handed) are reported below (mean age: 23; SD= 2.7).

Trial and Error Learning Task

The participants in this study were told that they would perform a trial-and-error learning task to map specific key presses to specific stimuli (digit codes) displayed on the computer screen. This task is a variant of the go/no go discrimination task developed by Newman et al. (1990). On each trial, one of sixteen two-digit codes (‘targets,’ e.g. 15, 23, 47) was presented on-screen (1500 ms maximum duration). Targets were randomly presented, with the constraint that the same target could not occur on consecutive trials. Half of these were pre-designated as ‘go’ stimuli; the other half was pre-designated as ‘nogo’ stimuli. On each trial, the participant had the opportunity to press one of four buttons on the keyboard (each button was associated with two unique two-digit numbers) mapped onto the index and middle fingers of their right and left hands), or to withhold a button-press response. The target was terminated when participants made a response or 1500 ms elapsed. After each response (or non-response), contingent feedback was immediately provided to the participant, who was asked to use that feedback to improve performance on future trials. The most important aspects of this task for the present study are that 1) the relation between the visual stimulus and motor response (or lack thereof for the no go trials) is arbitrary and causal (which defines arbitrary visuomotor association tasks and have been used extensively to study learning, see Wise & Murray, 2000) and 2) that the input (stimulus) to output mappings be consistent (for the development of expertise, see Chein & Schneider, 2005).

The error feedback could be of two forms: ‘ErrorGo’ indicated to the participant that a response was incorrectly performed on a ‘nogo’ trial, while ‘ErrorNG’ indicated that a response was not made on a ‘go’ trial. Correct feedback could, in turn, be of four forms: ‘Correct’ indicated that the response was correct (but with the wrong hand), ‘CorrectH’ indicated that the correct hand was used (but not the correct finger), ‘CorrectF’ indicated that the response was completely correct (hand and finger), and CorrectNG indicated that a response was correctly withheld on a ‘nogo’ trial. The feedback was presented for a maximum duration of 10 seconds, unless terminated by the subject with a button press. The inter-trial interval varied between 1500 and 2500 ms. There was a total of 800 trials and these were grouped into 100 trial blocks.

Participants were informed that correct feedback (CorrectNG and CorrectF) resulted in 8 points earned, Error feedback (ErrorGo and ErrorNG) results in 8 points lost, and partial correct feedback, Correct and CorrectH, result in loss of 4 and 2 points, respectively. Participants started the study with zero points. To motivate participants to learn the task, they were informed that their goal should be to earn as many points as possible because they will be paid a monetary

bonus according to the amount of points they accumulate by the end of the study. Participants were paid $15 for their participation and an additional amount, ranging between $25 and $45, depending on task performance. On average they earned $40 each. Between blocks, participants took a brief break and recorded their accumulated points on a form.

We used a 'fixed-number of consecutive correct responses' (FCCR) method for determining an individual learning threshold for each participant. In this method, the learning threshold is defined as the moment when participants made four consecutive correct responses (or withholding of a response) for a particular target.

EEG Recordings

A 128-channel HydroCel Geodesic Sensor Net (Electrical Geodesics, Inc., Eugene, OR) was used to record the EEG. Impedances were maintained below 70 kΩ (Ferree et al., 2001) during data acquisition. All recordings were sampled at 256 s/s (.1 to 100 Hz hardware filter) with a 16-bit analog-to-digital converter and referenced to Cz.

Procedure

Participants completed several mood questionnaires prior to the EEG recording not reported here. Once fitted with the 128-channel Hydrocel Geodesic Sensor Net, participants were seated 55 cm in front of the computer monitor. A chin rest was used to minimize head movements, and to maximize consistency of gaze alignment to the monitor. Prior to testing, participants performed a 32-trial practice session, during which they learned to associate the hand/finger mappings to 4 two-digit numbers. All showed proficiency at these finger mappings by the end of this practice session.

EEG Processing

The continuous EEG data were digitally filtered with a 30Hz low pass (finite impulse response) filter and then segmented relative to target and feedback onset. Each segment consisted of a 400 ms prestimulus baseline and extended for 1000 ms post stimulus. The segments were sorted according to accuracy (correct: includes trials containing CorrectNG and CorrectG feedback, error: includes trials containing ErrorGo and ErrorNG feedback) and whether they occurred prior to, or after, learning had been established (2 levels). Go and nogo trials were collapsed over accuracy and learning stage. Each segment of the EEG was excluded from signal averaging if 10 or more channels contained data that exceeded a voltage threshold of 200μV (absolute) or a transition threshold of 100 μV (sample to sample) or was contaminated by blinks. After averaging, the data was re-referenced to the average reference.

Source Estimates

Source estimates, describing the neural sources of the measured scalp potentials, were accomplished with the GeoSource electrial source imaging software (EGI, Eugene, OR, www.egi.com). GeoSource uses a finite difference model (FDM) for accurate computation of the lead field in relation to head tissues, where the primary resistive component is the skull. The FDM allows accurate characterization of the cranial orifices, primarily the optical canals and foramen magnum. Tissue compartments of the FDM were constructed from whole head MRI and CT scans of a single subject whose head shape closely matches the Montreal Neurologic Institute (MNI) average MRI. The MRI and CT images were co-registered prior to segmentation of the brain and cerebral spinal fluid (identified from MRI data), and the skull and scalp (identified from CT images), and the individual's MRI and CT images were aligned with the cortex volume from the MNI atlas with Talaraich registration. The tissue volumes were parceled using 2 mm voxels to form the computational elements of the FDM.

Conductivity values used in the FDM model are as follows: .25 S/m (Siemens/meter) for brain, 1.8 S/m for cerebral spinal fluid, .018 S/m for skull, and .44 S/m for scalp (see Ferree et al., 2000). These values reflect recent evidence that the skull-to-brain conductivity ratio is about 1:14, compared to the 1:80 ratio traditionally assumed (Ryynanen et al, 2006; Ryynanen et al, 2004, Zhang et al., 2006). With these more accurate conductivity values, the EEG may provide a spatial resolution equivalent to the magnetoencephalogram (MEG; Malmivuo & Suihko, 2004). Source locations were derived from the MNI probabilistic MRI (to which the typical subject matches closely). Based on the probabilistic map, gray matter volume was parceled into 7 mm voxels, each voxel served as a source location with three orthogonal orientations. This resulted in a total of 2,394 sources whose anatomic identity was derived through use of a Talaraich demon (Lancaster et al., 2000). The source locations were registered with the MRI and CT volumes. Once the head model was constructed, an average of the 128-channel sensor positions was registered to the scalp surface. To compute estimates of the sources, a minimum norm solution with the LAURA (local autoregressive average) constraint (Grave de Peralta Menendez et al., 2004) was used. All source estimates were performed on the grand-averaged scalp data.

Acknowledgements

This project was supported by the Office of Naval Research HPT&E and VIRTE programs and NIMH grant MH070911.

References

Badre D, Poldrack RA, Paré-Blagoev J, Insler RZ, Wagner AD. Dissociable controlled retrieval and generalized selection mechanisms in ventrolateral prefrontal cortex. Neuron 2005;47:907–918. [PubMed: 16157284]

Barceló F, Muñoz-Céspedes JM, Pozo MA, Rubia FJ. Attentional set shifting modulates the target p3b response in the wisconsin card sorting test. Neuropsychologia 2000;38:1342–1355. [PubMed: 10869577]

Behrens TEJ, Woolrich MW, Walton ME, Rushworth MFS. Learning the value of information in an uncertain world. Nature Neuroscience 2007;10:1214–1221.

Botvinick MW, Cohen JD, Carter CS. Conflict monitoring and anterior cingulate cortex: and update. Trends in Cognitive Sciences 2004;8:539–546. [PubMed: 15556023]

Bunge SA, Kahn I, Wallis JD, Miller EK, Wagner AD. Neural circuits subserving the retrieval and maintenance of abstract rules. Journal of Neurophysiology 2003;90:3419–3428. [PubMed: 12867532]

Bussey TJ, Wise SP, Murray EA. The role of ventral and orbital prefrontal cortex in conditional visuomotor learning and strategy use in rhesus monkeys (macaca mulatta). Behavioral Neuroscience 2001;115:971–982. [PubMed: 11584930]

Bussey TJ, Wise SP, Murray EA. Interaction of ventral and orbital prefrontal cortex with inferotemporal cortex in conditional visuomotor learning. Behavioral Neuroscience 2002;116:703–715. [PubMed: 12148937]

Chein JM, Schneider W. Neuroimaging studies of practice-related change: Fmri and meta-analytic evidence of a domain general control network for learning. Cognitive Brain Research 2005;25:607–623. [PubMed: 16242923]

Donchin E, Coles MGH. Is the p300 component a manifestation of context updating? Behavioral and Brain Sciences 1988;11:357–374.

Eliassen JC, Souza T, Sanes JN. Experience-dependent activation patterns in human brain during visual-motor associative learning. Journal of Neuroscience 2003;23(33):10540–10547. [PubMed: 14627638]

Elliott R, Dolan RJ. Activation of different anterior cingulate foci in association with hypothesis testing and response selection. Neuroimage 1998;8:17–29. [PubMed: 9698572]

Gabriel, M.; Burhans, L.; Talk, A.; Scalf, P. Cingulate cortex. In: Ramachandran, VS., editor. Encyclopedia of the human brain. Elsevier Science; 2002. p. 775-791.

Gehring WJ, Willoughby AR. The medial frontal cortex and the rapid processing of monetary gains and losses. Science 2002;295:2279–2282. [PubMed: 11910116]

Goldberg G. Supplementary motor area structure and function: Review and hypotheses. Behavioral and Brain Sciences 1985;8:567–615.

Gonsalvez CJ, Gordon E, Grayson S, Barry RJ, Lazzaro I, Bahramali H. Is the target-to-target interval a critical determinant of P3 amplitude? Psychophysiology 1999;36(5):643–654. [PubMed: 10442033]

Gonsalvez CL, Polich J. P300 amplitude is determined by target-to-target interval. Psychophysiology 2002;39(3):388–396. [PubMed: 12212658]

Grave de Peralta Menendez R, Murray MM, Michel CM, Martuzzi R, Gonzalez Andino SL. Electrical neuroimaging based on biophysical constraints. Neuroimage 2004;21:527–539. [PubMed: 14980555]

Hajcak G, Holroyd CB, Moser JS, Simons RF. Brain potentials associated with expected and unexpected good and bad outcomes. Psychophysiology 2005;42:161–170. [PubMed: 15787853]

Holroyd CB, Coles MGH. The basis of human error processing: Reinforcement learning, dopamine, and the error-related negativity. Psychological Review 2002;109:679–709. [PubMed: 12374324]

Holroyd CB, Nieuwenhuis S, Yeung N, Nystrom L, Mars RB, Coles MGH, et al. Dorsal anterior cingulate cortex shows fmri response to internal and external error signals. Nature Neuroscience 2004;7:497–498.

Keng E, Gabriel M. Hippocampal modulation of cingulo-thalamic neuronal activity and discriminative avoidance learning in rabbits. Hippocampus 1998;8:491–510. [PubMed: 9825960]

Kiehl KA, Liddle PF, Hopfinger JB. Error processing and the rostral anterior cingulate: An event-related fmri study. Psychophysiology 2000;37:216–223. [PubMed: 10731771]

Kotchobey B, Grözinger B, Kornhuber AW, Kornhuber HH. Electrophysiological analysis of expectancy: P3 in informed guessing. International Journal of Neuroscience 1997;91:291–308.

Lancaster JL, Woldorff MG, Parsons LM, Liotti M, Freitas CS, Rainey L, Kochunov PV, Nickerson D, Mikiten SA, Fox PT. Automated Talairach Atlas labels for functional brain mapping. Human Brain Mapping 2000;10:120–131. [PubMed: 10912591]

Luu, P.; Tucker, DM. Self-regulation and the executive functions: Electrophysiological clues. In: Zani, A.; Preverbio, AM., editors. The cognitive electrophysiology of mind and brain. San Diego: Academic Press; 2003. p. 199-223.

Luu P, Tucker DM, Derryberry D, Reed M, Poulsen C. Electrophysiological responses to errors and feedback in the process of action regulation. Psychological Science 2003;14:47–53. [PubMed: 12564753]

Luu P, Tucker DM, Makeig S. Frontal midline theta and the error-related negativity: Neurophysiological mechanisms of action regulation. Clinical Neurophysiology 2004;115:1821–1835. [PubMed: 15261861]

Luu P, Tucker DM, Stripling R. Neural mechanisms for learning actions in context. Brain Research 2007;1179:89–105. [PubMed: 17936726]

Malmivuo JA, Suihko VE. Effect of skull resistivity on the spatial resolutions of EEG and MEG. IEEE Transactions on Biomedical Engineering 2004;51:1276–1280. [PubMed: 15248545]

Menon V, Adleman NE, White CD, Glover GH, Reiss AL. Error-related brain activation during a go/nogo response inhibition task. Human Brain Mapping 2001;12:131–143. [PubMed: 11170305]

Mishkin M. A memory system in the monkey. Philosophical Transactions of the Royal Society of London: Series B 1982;298:85–95.

Müller SV, Möller J, Rodriguez-Fornells A, Münte TF. Brain potentials related to self-generated and external information used for performance monitoring. Clinical Neurophysiology 2005;116:63–74. [PubMed: 15589185]

Newman JP, Patterson MC, Howland EW, Nichols SL. Passive avoidance in psychopaths: the effects of reward. Personality and Individual Differences 1990;11:1101–1114.

Passingham RE, Toni I, Rushworth MF. Specialisation within the prefrontal cortex: the ventral prefrontal cortex and associative learning. Experimental Brain Research 2000;133:103–113.

Poldrack RA, Sabb FW, Foerde K, Tom SM, Asarnow RF, Bookheimer SY, et al. The neural correlates of motor skill automaticity. Journal of Neuroscience 2005;25:536–5364.

Rushworth MFS, Walton ME, Kennerley SW, Bannerman DM. Action sets and decisions in the medial frontal cortex. Trends in Cognitive Sciences 2004;8:410–417. [PubMed: 15350242]

Ryynanen OR, Hyttinen JA, Laarne PH, Malmivuo JA. Effect of electrode density and measurement noise on the spatial resolution of cortical potential distribution. IEEE Transactions in Biomedical Engineering 2004;51:1547–1554.

Ryynanen OR, Hyttinen JA, Malmivuo JA. Effect of measurement noise and electrode density on the spatial resolution of cortical potential distribution with different resistivity values for the skull. IEEE Transactions in Biomedical Engineering 2006;53:1851–1858.

Segalowitz N, Segalowitz SJ. Skilled performance, practice, and the differentiation of speed-up from automatization effects: Evidence from second language word recognition. Applied Psycholinguistics 1993;14:369–385.

Simons JS, Spiers HJ. Prefrontal and medial temporal lobe interactions in long-term memory. Nature Reviews Neuroscience 2003;4:637–648.

Somerville L, Heatherton TF, Kelley WM. Anterior cingulate cortex responds differentially to expectancy violation and social rejection. Nature Neuroscience 2006;9:1007–1008.

Toni I, Krams M, Turner R, Passingham RE. The time course of changes during motor sequence learning: A whole-brain fMRI study. Neuroimage 1998;8:50–61. [PubMed: 9698575]

Toni I, Ramnani N, Josephs O, Ashburner J, Passingham RE. Learning arbitrary visuomotor associations: Temporal dynamic of brain activity. Neuroimage 2001;14:1048–1057. [PubMed: 11697936]

Tucker, DM.; Luu, P. Adaptive binding. In: Zimmer, H.; Mecklinger, A.; Linden-berger, U., editors. Binding in human memory: A neurocognitive approach. New York: Oxford University Press; 2006. p. 85-113.

Tucker DM, Luu P. Neurophysiology of motivated learning: Adaptive mechanisms underlying cognitive bias in depression. Cognitive Therapy and Research 2007;31:189–209.

Ullsperger M, von Cramon DY. Error monitoring using external feedback: Specific roles of the habenular complex, the reward system, and the cingulate motor area revealed by functional magnetic resonance imaging. Journal of Neuroscience 2003;23:4308–4314. [PubMed: 12764119]

Wilcox, RR. Introduction to robust estimation and hypothesis testing. San Diego: Academic; 1997.

Wise SP, Murray EA. Arbitrary associations between antecedents and actions. Trends in Neurosciences 2000;23:271–276. [PubMed: 10838597]

Zhang Y, van Drongelen W, He B. Estimation of in-vivo brain-to-skull conductivity ration in humans. Applied Physics Letters 2006;89:223903–3. [PubMed: 17492058]

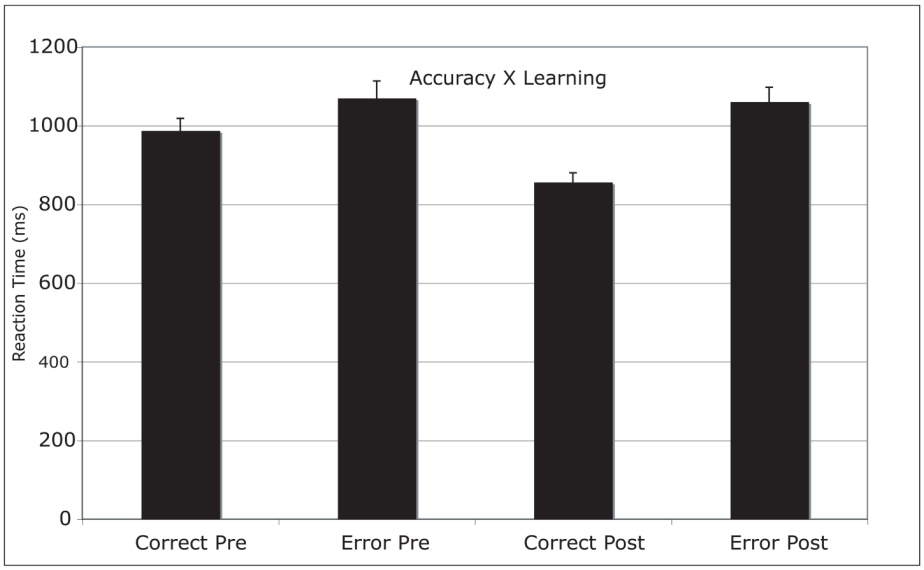

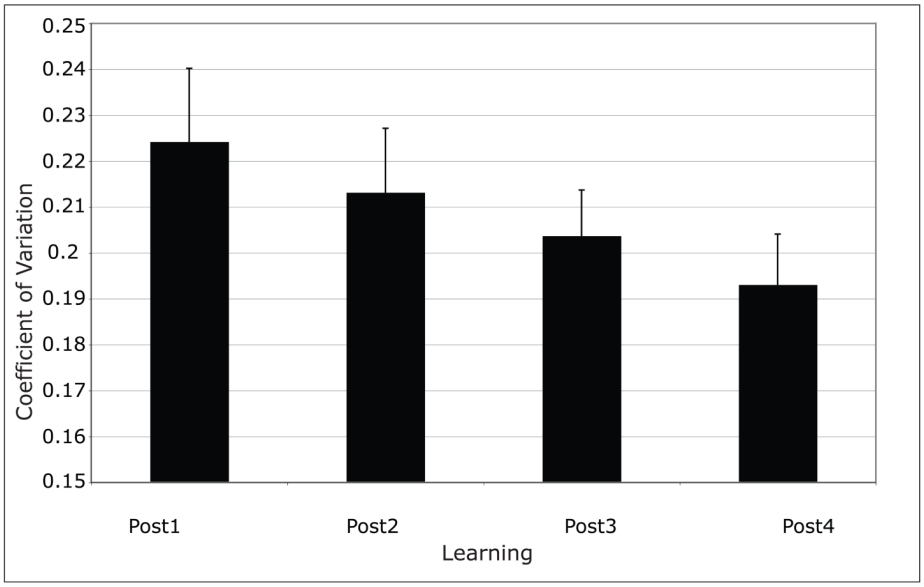

Figure 1.
Reaction time (Accuracy × Learning interaction) and coefficient of variation (CV) graphs.

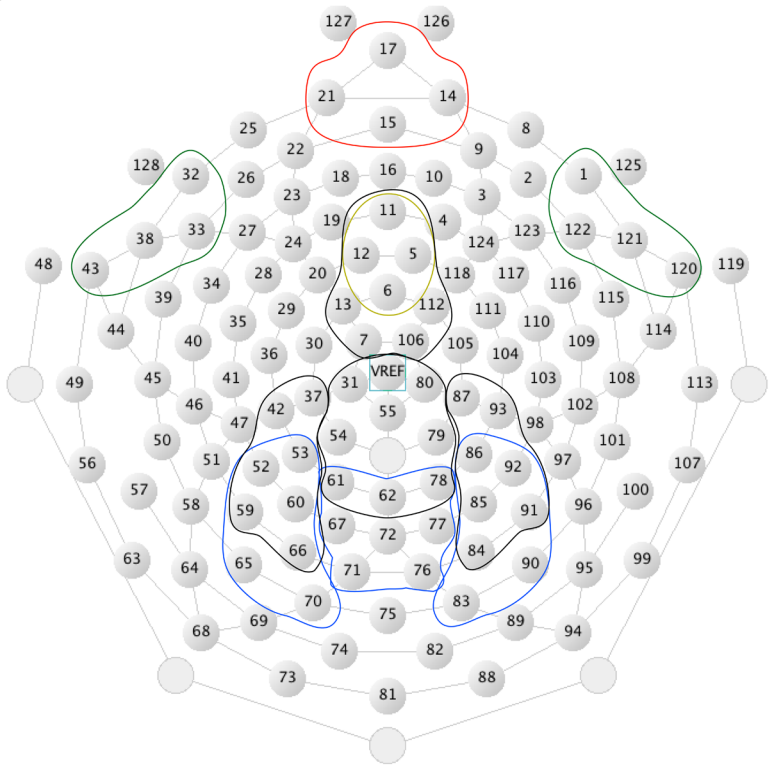

Figure 2.
Layout of Hydrocel Geodesic Sensor Net and channel groups used for analysis. Orange: FRN; Yellow: MFN; Green: LIAN; Black: Feedback-locked P3; Blue: Target-locked P3.

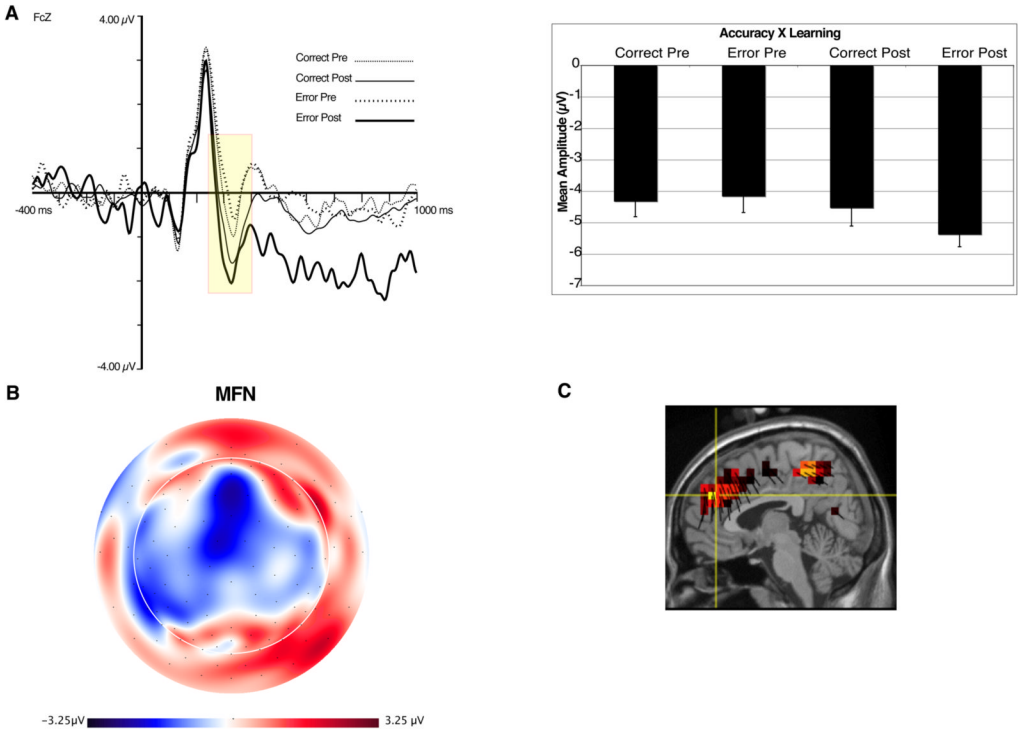

Figure 3.

A. ERP waveforms at site FCz (left). Yellow box represents time window used for quantification of the MFN. Accuracy × Learning interaction for MFN (right). B. Topographic map of difference between post- and pre-error trials, at 300 ms. Orientation of map is top looking down with nose at top of page. C. Source distribution for MFN, also at 300 ms.

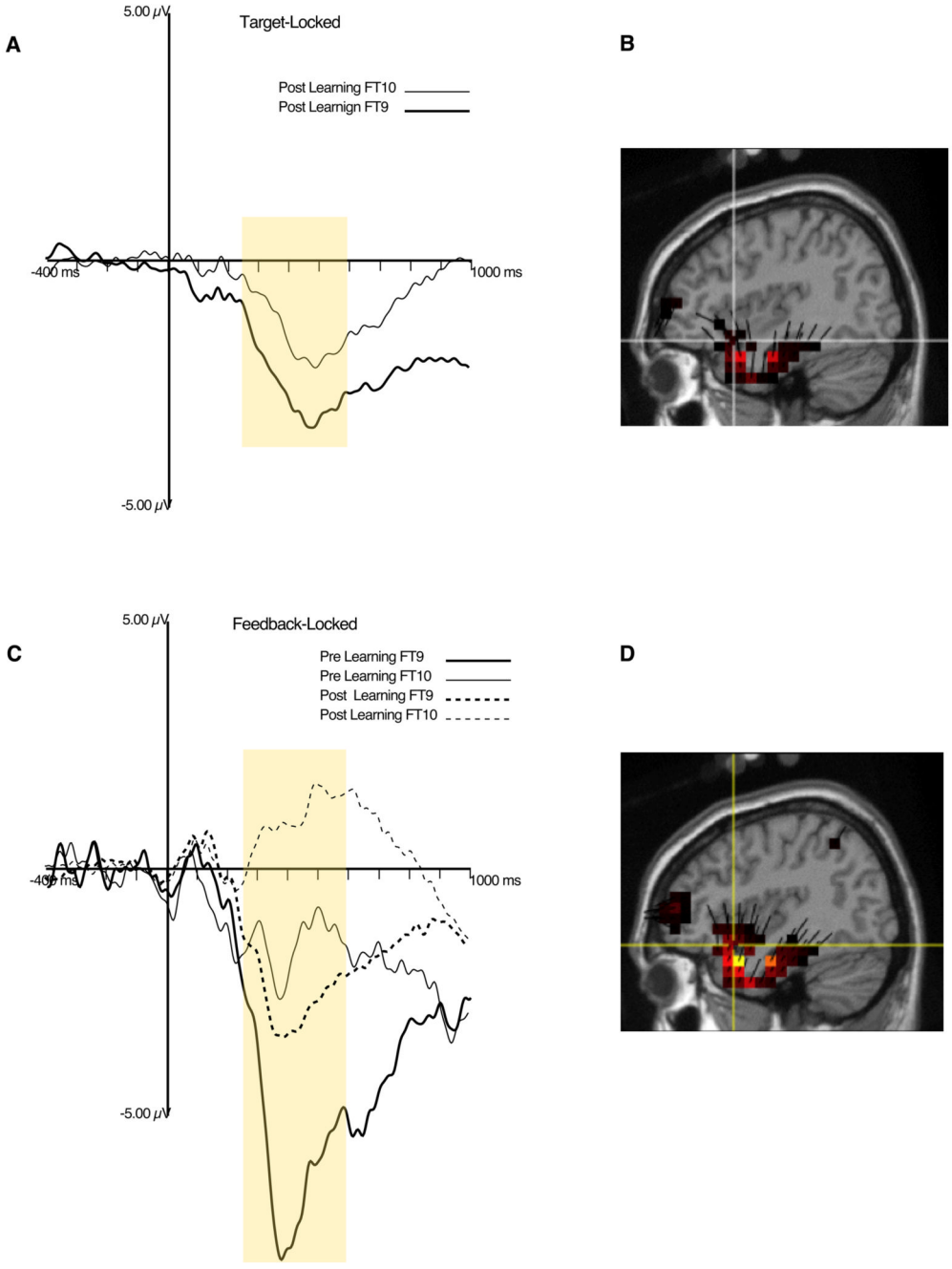

Figure 4.

A. ERP waveforms plot of target-locked LIAN. Yellow box represents time window used for quantification of the LIAN. B. Source distribution for target-locked LIAN, at the maximum amplitude point, using data from the condition with the largest response (pre-learning). C. ERP waveform plot of feedback-locked LIAN. Yellow box represents time window used for quantification of the LIAN. D. Source distribution for feedback-locked LIAN, also at the maximum amplitude point, with data from the condition with the largest response (post-learning).

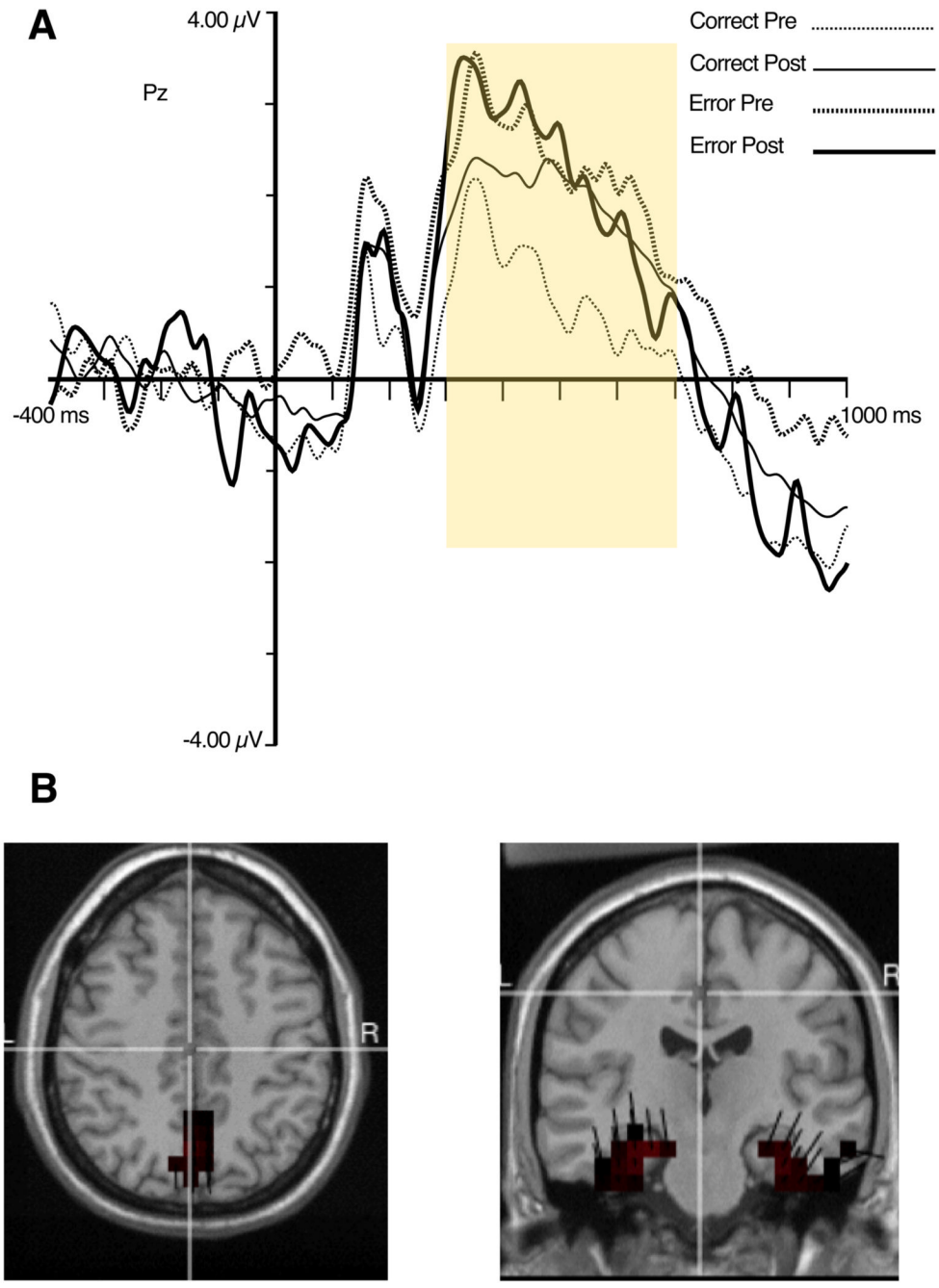

Figure 5.

A. ERP waveforms for target-locked P3 at site Pz. Yellow box represents time window used for quantification of the P3. B. Source distribution of P3.

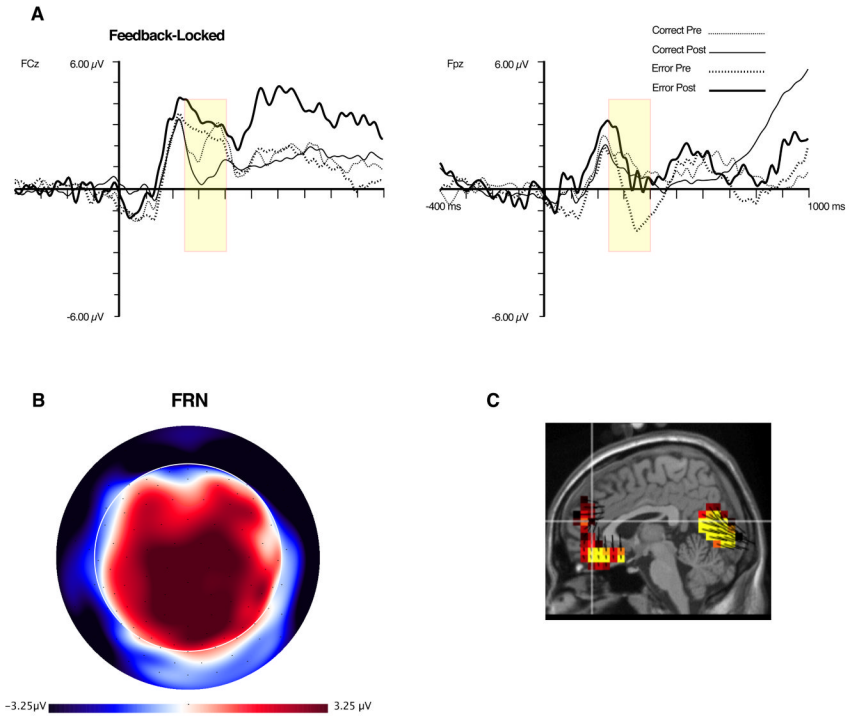

Figure 6.

A. ERP waveform for FRN at sites FCz and Fpz. Yellow box represents time window used for quantification of the FRN. B. Topographic map of difference between pre-error and post-correct trials, at 350 ms. Orientation of map is top looking down with nose at top of page. C. Source distribution for FRN, also at 350 ms.

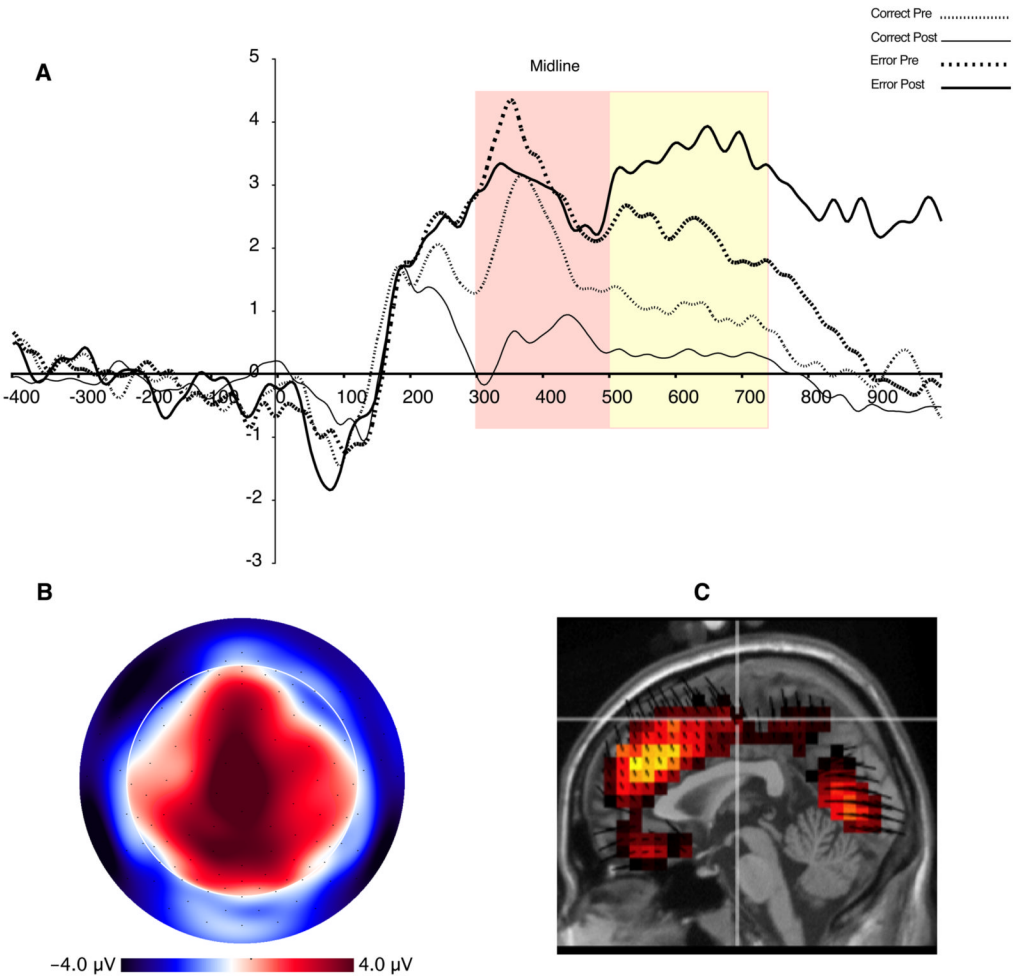

Figure 7.

ERP waveforms for feedback-locked P3 averaged over medioparietal sites (see Figure 3). Red and yellow boxes represent time window used for quantification of $P3_1$ and P_2, respectively. B. Topographic map illustrating $P3_2$ distribution at 680 ms. Orientation of map is top looking down with nose at top of page. C. Source distribution for $P3_s$, also at 680 ms.